

ENDURANCE EVALUATION OF DIFFERENT UAV CONFIGURATIONS AND POWERTRAIN ARCHITECTURES

Antonio ORGIU[1,2], Scott DELBECQ[1] & Jonathan LISCOUËT[2]

[1]ISAE-SUPAERO, Université de Toulouse, Toulouse, France
[2]Concordia University, Montréal, Canada

DOI: 10.71945/icas2026_0636

Abstract

Unmanned Aerial Vehicles (UAVs) are increasingly central to modern aerospace engineering. Traditional UAV design relies on sequential and iterative approaches, which manage interdisciplinary interactions through manual coordination and repeated adjustments, often leading to long development cycles and locally optimal solutions and perform sensitivity studies with respect to novel architectures and changes in requirements. This leads to a lack of comparative studies of UAV architectures and sensitivities to requirements and technological assumptions. This paper proposes to use FAST-UAV, an open source Multidisciplinary Design Analysis and Optimization framework for the preliminary design of UAVs. To this end, a thermal propulsion modeling strategy for fixed-wing and hybrid Vertical take-Off and landing UAVs is added to the framework. The latter is then used to systematically compare endurance across UAV architectures, maximum vehicle mass, and payloads. Results illustrate significant endurance variations and ranking between electric and thermal propulsion systems, highlighting the potential of this approach to support informed preliminary design decisions across diverse UAV mission scenarios.

Keywords: UAV design - MDAO - Thermal propulsion - Endurance analysis - Preliminary design

Introduction

Unmanned Aerial Vehicles (UAVs) have become a cornerstone of modern aerospace engineering, enabling a wide range of civil and military applications due to their versatility, reduced operational costs, and increasing autonomy and maneuvrability. Their design has traditionally relied on sequential and iterative methodologies, in which all disciplines are addressed in a staged manner. In practice, interdisciplinary couplings are generally managed through iterative adjustments, rather than through an explicit system-level formulation, resulting in long development cycles and strongly based on the experience and personal judgment of engineers [1, 2]. Multidisciplinary Design Analysis and Optimization (MDAO) overcomes these limitations by explicitly solving multiple strongly coupled interacting disciplines within a unified mathematical framework, enabling an efficient exploration of high-dimensional design spaces and the identification of system-level optimal UAV configurations.
While a substantial number of studies have applied MDAO to UAV design, existing literature predominantly focuses on electrically propelled and multirotor platforms intended for short-range missions [3, 4, 5, 6, 7]. Although this emphasis is consistent with current industrial trends and regulatory considerations, Internal Combustion Engines (ICEs) remain a relevant propulsion option across a broad range of UAV classes, particularly for endurance- and range-oriented missions, owing to their high power and energy density. However, to the authors' knowledge, their integration as fully coupled disciplines within system-level MDO formulations appears to be relatively unexplored in the literature. This gap also limits consistent comparisons between electric and thermal propulsion architectures at

the preliminary design stage, thereby constraining the assessment of the most suitable propulsion solution for a given mission profile. This study is restricted to the small-UAV regulatory class, i.e. a maximum take-off mass (MTOM) of $25\,\mathrm{kg}$. This threshold is the ceiling of the EASA "Open" category [8] and, equivalently, of the FAA Part 107 small-UAS rule [9] ($55\,\mathrm{lb} \quad 25\,\mathrm{kg}$). It is the regime for which the FAST-UAV disciplinary models are calibrated, and it bounds the design space considered throughout this work. The present work proposes an application of the MDO framework for thermal propulsion, focusing on the systematic comparison of UAV endurance across different architectures, including fixed-wing and hybrid VTOL configurations, for varying vehicle sizes, propulsion types, and payloads.

The paper is organized in four main sections. The first one provides a short overview of the FAST-UAV framework, along with the description of the adopted MDO architecture of the problem. The second section describes the implementation of thermal propulsion within a dedicated MDO framework, detailing the model that has been used and their integration as a fully coupled discipline. In the third section the evaluation of UAV endurance across different vehicle architectures, sizes, and propulsion types is presented. The final section concludes the report, highlighting the main findings and areas for improvement.

1. FAST-UAV

The practical application of MDO relies on dedicated Multidisciplinary Design Analysis and Optimization (MDAO) frameworks, which provide the computational tools required to formulate and solve complex design problems. These frameworks differ in terms of supported MDO architectures and optimizers, and they are suitable to handle the large-scale, heterogeneous models that typically arise in aerospace system design. Among these frameworks, OpenMDAO, developed at NASA, is a widely adopted open source Python package for MDAO problems [10]. Built upon this foundation, FAST-OAD is a framework developed by ONERA and ISAE-SUPAERO for overall aircraft design, which provides a structured and aeronautics-specific MDAO environment for conceptual and preliminary design-related studies [11].

Extending FAST-OAD towards the specific requirements of UAV design, FAST-UAV has been developed by INSA Toulouse, ISAE-SUPAERO and Concordia University to introduce UAV-oriented disciplinary models, sizing logics, and mission formulations. FAST-UAV therefore provides a modular and extensible Python-based environment tailored to UAV conceptual and preliminary design, while retaining the underlying OpenMDAO capabilities for gradient-based optimization and support of multiple MDO architectures. All the model formulations used for structural analysis, aerodynamics, and electric propulsion, as well as their validation, are described in detail in [3, 4]. In its current state (prior to the contribution presented in this article), FAST-UAV supports the design of multirotor, fixed-wing, and hybrid-VTOL vehicles, all of which are exclusively electric-powered.

All the disciplines are integrated within FAST-UAV using an hybrid MDO formulation proposed by [12, 13], called the Normalized Variable Hybrid (NVH). This formulation takes inspiration from the work of [14], who proposed an IDF-like (Individual Design Feasible) architecture where the feedforward consistency is achieved by solving the discipline modules in sequence; instead the feedback consistency is always linked to the optimizer, as in the classical IDF configuration. NHV adopts this architecture but modifying the definition of the one coupling variable, expressing it as a multiple of a known quantity [4, 12, 13, 15]:

$$y = k \cdot y_0 \tag{1}$$

where y_0 is a known quantity, k is the normalized design variable from the optimizer, and y is the obtained coupling variable. For example, in the current implementation on FAST-UAV, the design variable related to the MTOW of the UAV is not its absolute value, but the coefficient k multiplying the payload mass. An advantage of this formulation is that, for the most part of the problems, the values for k do not go outside the interval $[0.1, 10.0]$ and makes the code generic for any UAV size as initial guesses scale with the requirements. Reducing the dimension of the design variables, the optimizer improves its numerical solution accuracy and its ability to achieve convergence [13, 15].

2. Expanding FAST-UAV towards internal combustion engines

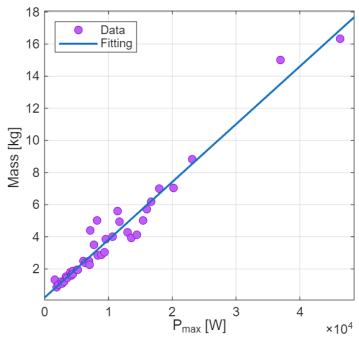
This section extends the FAST-UAV multidisciplinary design optimization framework to Internal Combustion Engine (ICE) propulsion. A set of data regression models, constructed from a dataset of two-stroke UAV engines, is developed to estimate the main geometric and performance parameters from a minimal set of design drivers. The following subsections detail the regression models and their statistical characterization, the implementation within the FAST-UAV sizing architecture.

2.1 Models for ICEs

The internal combustion engine module implemented within FAST-UAV relies primarily on data regression models. These are constructed using data collected from manufacturer catalogs of engines specifically developed for UAVs, namely 3W–Motoren und Flugmodelle, SKYPOWER International, HFE International, DLE, HIRT Engines, Limbach Flugmotoren, Currawong Engineering, and Rotron Power. The dataset includes only two-stroke ICEs, represented in single-, two-, and four-cylinder configurations, with maximum power ranging from $1.6\,\mathrm{kW}$ to $46.3\,\mathrm{kW}$. Multicylinder engines are considered exclusively in horizontal configurations, i.e. opposed or boxer, as this layout represents the most widely adopted solution in the current UAV and ultralight aircraft engine market.

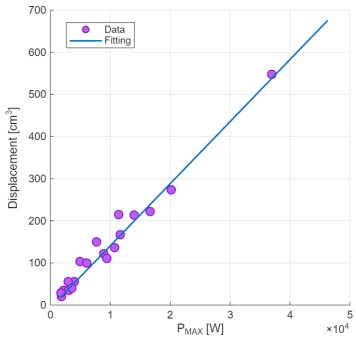
The regression-based models are used to estimate the main geometric and performance parameters characterizing an internal combustion engine, starting from a limited set of design drivers, such as the maximum power or a reference length. This enables a compact yet flexible representation suitable for preliminary design studies.

Linear regression models relating engine mass, displacement, and maximum torque to maximum power output are shown in Figure 1. All three models exhibit strong linear correlations, with R-squared values of 0.9615, 0.9703, and 0.9843, respectively. Overall, the results confirm that simple linear regression provides an effective first-order approximation for the considered engine parameters within the observed power range.



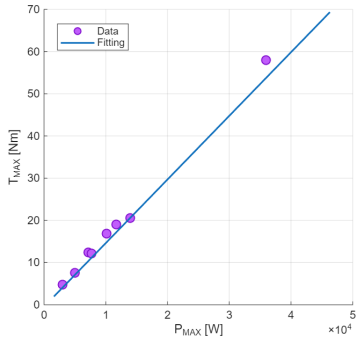
(a) Weight vs P_{MAX}

Statistic	Value
R-square	0.9615
RMSE	0.6591



(b) Displacement vs P_{MAX}

Statistic	Value
R-square	0.9703
RMSE	21.77



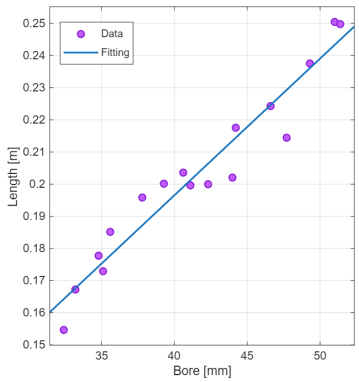
(c) T_{MAX} vs P_{MAX}

Statistic	Value
R-square	0.9843
RMSE	5.09

Figure 1 – Linear regression models of engine parameters as a function of maximum power output.

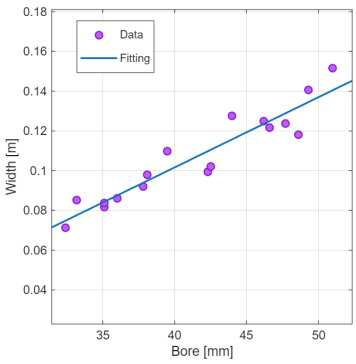
Figures 2 and 3 present linear regression models for the three main engine dimensions, length, width, and height, as a function of cylinder bore, for single-cylinder and multi-cylinder engines, respectively. The rationale behind this choice of independent variable lies in the fact that the overall envelope dimensions of piston engines are primarily driven by multiples of the cylinder bore diameter. For single-cylinder engines, length and width exhibit strong linear correlations, with R-squared values of 0.9349 and 0.9550, respectively. The height model, however, shows a comparatively lower R-squared of 0.89045, suggesting that vertical dimensions are more sensitive to design-specific factors such as intake and exhaust manifold routing, cylinder head geometry, or accessory stacking. Multi-cylinder engines show comparable or slightly higher R-squared values of 0.9634, 0.9852, and 0.9676, though with notably larger Root Mean Square Error (RMSE) values, reflecting the greater dimensional

variability inherent in multi-cylinder configurations. The reduced scatter in the single-cylinder data can be attributed to their simpler and more constrained packaging, whereas the larger residuals in multi-cylinder models arise from manufacturer-specific design choices (accessory placement, cooling layout, crankcase design etc.) not captured by bore alone. Overall, these results confirm that cylinder bore can be effectively used as a single design parameter to estimate the principal dimensions of both engine classes.



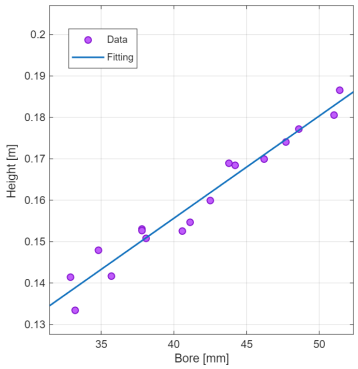
(a) Length vs Bore

Statistic	Value
R-square	0.9349
RMSE	7.2114



(b) Width vs Bore

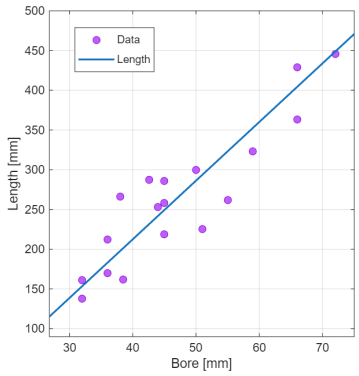
Statistic	Value
R-square	0.9550
RMSE	3.3319



(c) Height vs Bore

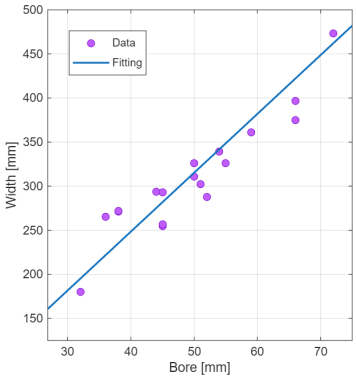
Statistic	Value
R-square	0.89045
RMSE	7.7766

Figure 2 – Linear regression models of engine dimensions, for single-cylinder engines, as a function of the bore of the cylinder.



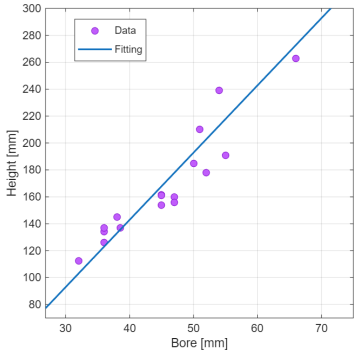
(a) Length vs Bore

Statistic	Value
R-square	0.9634
RMSE	44.540



(b) Width vs Bore

Statistic	Value
R-square	0.9852
RMSE	29.596



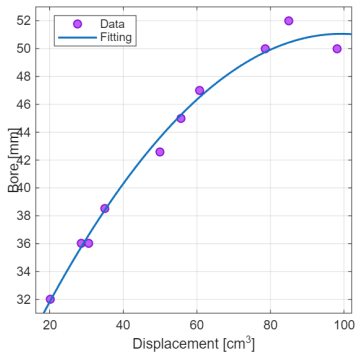
(c) Height vs Bore

Statistic	Value
R-square	0.9676
RMSE	29.603

Figure 3 – Linear regression models of engine dimensions, for multi-cylinder engines, as a function of the bore of the cylinder.

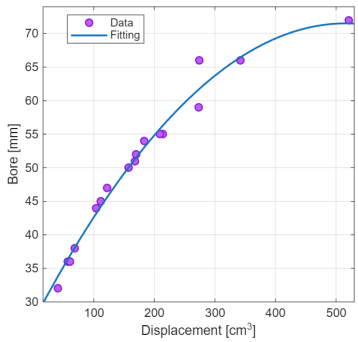
To conclude, Figure 4 and Figure 5 present the regression models relating cylinder bore and stroke to engine displacement for each subcategory (single-, two-, and four-cylinder). A second-order polynomial was selected for the bore-displacement relationship, consistent with the quadratic dependence of bore on cylinder volume ($V \propto B^2$), while a linear model was adopted for stroke, which scales linearly with displacement at constant bore. The resulting fits exhibit strong predictive capability across single- and two-cylinders configurations, with R-squared values exceeding 0.91 and RMSE values remaining within acceptable bounds relative to the observed data ranges. The four-cylinders subcategory, while still yielding high R-squared values, is represented by a comparatively limited sample

size, which reduces the statistical robustness of the corresponding models and may affect their generalizability beyond the observed displacement range. Expanding this subset in future work would help consolidate the preliminary trends identified here.



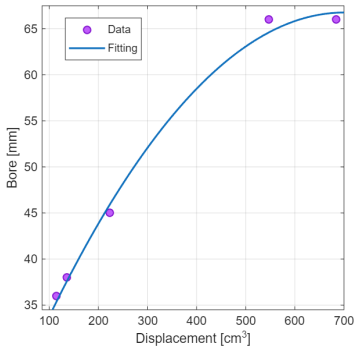
(a) Bore vs Displacement (single-cylinder)

Statistic	Value
R-square	0.9893
RMSE	0.7208



(b) Bore vs Displacement (two-cylinders)

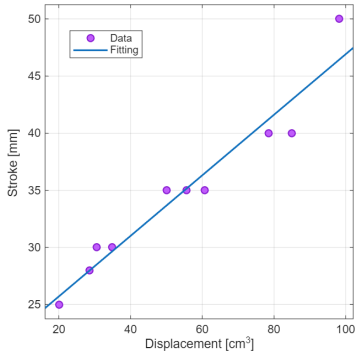
Statistic	Value
R-square	0.9808
RMSE	1.5276



(c) Bore vs Displacement (four-cylinders)

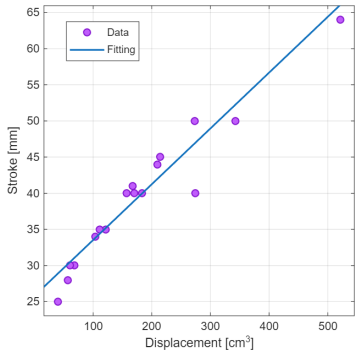
Statistic	Value
R-square	0.9949
RMSE	1.2417

Figure 4 – Linear regression models of engine bore, for single-, two-, and four-cylinders engines, as a function of the displacement.



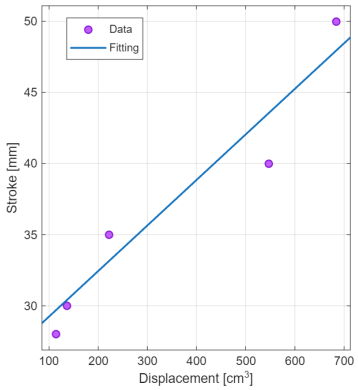
(a) Stroke vs Displacement (single-cylinder)

Statistic	Value
R-square	0.9461
RMSE	1.5768



(b) Stroke vs Displacement (two-cylinders)

Statistic	Value
R-square	0.9257
RMSE	2.5003



(c) Stroke vs Displacement (four-cylinders)

Statistic	Value
R-square	0.9150
RMSE	2.5811

Figure 5 – Linear regression models of engine stroke, for single-, two-, and four-cylinders engines, as a function of the displacement.

Table 1 summarises the regression models developed for the estimation of the main ICE parameters. For each model, the table reports the analytical expression with the corresponding numerical coefficients. All linear models follow the general form $y = ax + b$, while a second-order polynomial $y = ax^2 + bx + c$ is adopted for the bore-displacement relationship.

Table 1 – Summary of regression models for ICE parameters estimation.

Dependent variable	Independent variable	Model
Engine parameters vs maximum power		
Mass [kg]	$1.6{\cdot}10^3 \leq P_{\mathrm{MAX}} \leq 46.3{\cdot}10^3$ [W]	$m = 0.0004\,P_{\mathrm{MAX}} + 0.2090$
Displacement [cm^3]		$V_d = 0.0147\,P_{\mathrm{MAX}} - 6.7410$
T_{MAX} [N m]		$T_{\mathrm{MAX}} = 0.0015\,P_{\mathrm{MAX}} - 0.4529$
Engine dimensions vs cylinder bore (single-cylinder)		
Length [mm]	$32.4 \leq B \leq 51.4$ [mm]	$L = 4.2532\,B + 26.3811$
Width [mm]		$W = 3.5362\,B - 39.7119$
Height [mm]		$H = 2.4717\,B + 56.8445$
Engine dimensions vs cylinder bore (multi-cylinder)		
Length [mm]	$32.0 \leq B \leq 72.0$ [mm]	$L = 7.3853\,B - 83.0116$
Width [mm]		$W = 6.6735\,B - 18.4421$
Height [mm]		$H = 4.9931\,B - 56.7921$
Bore vs displacement (by cylinder count)		
Bore [mm] (1-cyl)	$20.1 \leq V_d \leq 98.1$ [cm^3]	$B = -0.0031\,V_d^2 + 0.6080\,V_d + 20.8803$
Bore [mm] (2-cyl)	$40.2 \leq V_d \leq 521.2$ [cm^3]	$B = -0.0002\,V_d^2 + 0.1722\,V_d + 27.0835$
Bore [mm] (4-cyl)	$114.0 \leq V_d \leq 648.2$ [cm^3]	$B = -0.0001\,V_d^2 + 0.1280\,V_d + 21.8843$
Stroke vs displacement (by cylinder count)		
Stroke [mm] (1-cyl)	$20.1 \leq V_d \leq 98.1$ [cm^3]	$S = 0.2652\,V_d + 20.3972$
Stroke [mm] (2-cyl)	$40.2 \leq V_d \leq 521.2$ [cm^3]	$S = 0.0772\,V_d + 25.8001$
Stroke [mm] (4-cyl)	$114.0 \leq V_d \leq 648.2$ [cm^3]	$S = 0.0320\,V_d + 26.0486$

2.2 Implementation on FAST-UAV

This section details how the regression-based models presented previously have been implemented within the FAST-UAV framework.

2.2.1 Engine module

The propulsion module contains the engine module, which implements the regression-based models showed before.

The engine module takes three inputs: N_{cyl}, RPC, and k_{eng}. The first two are integer parameters, while k_{eng} is a design variable governed by the optimizer. N_{cyl} denotes the desired number of cylinders (one, two, or four), and RPC (Rotations Per Cycle) indicates the number of active rotations per active engine cycle, essentially allowing the user to choose between 2-stroke ($RPC = 1$) and 4-stroke ($RPC = 2$) engines. As mentioned previously, only 2-stroke engines can be selected at this stage. Finally, the design variable k_{eng} ($\in [0,1]$) determines the maximum engine brake power according to the following relationship:

$$P_{b,MAX} = P_{lim,min} + k_{eng}(P_{lim,max} - P_{lim,min}) \tag{2}$$

The limits $P_{lim,min}$ and $P_{lim,max}$ correspond to those of the data regression models: $1.6\,\mathrm{kW}$ and $46.3\,\mathrm{kW}$, respectively. As shown previously, all the other engine characteristics can be determined by using the maximum power as the sole design parameter.

The fuel mass flow rate for each mission phase is computed from the maximum power using the following relationship:

$$\dot{m}_{f,phase} = \frac{P_{corr,phase}}{\eta_{fi}\,\eta_m\,H_{LHV}} \tag{3}$$

where $P_{corr,phase}$ is the brake power, for each mission phase, corrected for altitude-induced power loss according to the Gagg–Ferrar model [16]:

$$P_{corr,phase} = P_{b,phase} \frac{0.883}{(\sigma - 0.117)} \tag{4}$$

where σ is equal to the density ratio at altitude and at sea-level.
In 3, η_{fi} and η_m denote the fuel-indicated and mechanical efficiencies of the engine. Both are treated as constants, with $\eta_{fi} = 0.20$ and $\eta_m = 0.75$, yielding an overall fuel-to-brake conversion efficiency $\eta_{fi}\,\eta_m \approx 0.15$, i.e. a brake specific fuel consumption of about $545\,\mathrm{g/kWh}$. This value reflects the markedly lower brake efficiencies measured on small two-stroke gasoline engines in the considered size class (1.6–$46\,\mathrm{kW}$), as reported in [17, 18, 19, 20, 21]; the volumetric efficiency ($\eta_v = 0.75$ for the naturally-aspirated two-stroke) characterises the air charge / attainable power for a given displacement rather than the fuel-to-brake conversion, and is therefore not applied to the fuel mass flow (it is computed but does not enter the sizing). The lower heating value adopted corresponds to MOGAS/AVGAS fuel ($44\,\mathrm{MJ/kg}$).

2.2.2 Geometry constraints

To accomodate a thermal propulsion systems, the fuselage volume constraint has been adapted to account for the engine and fuel tank volumes. Figure 6 shows the internal layout of the engine, payload, and fuel tank within the fuselage.

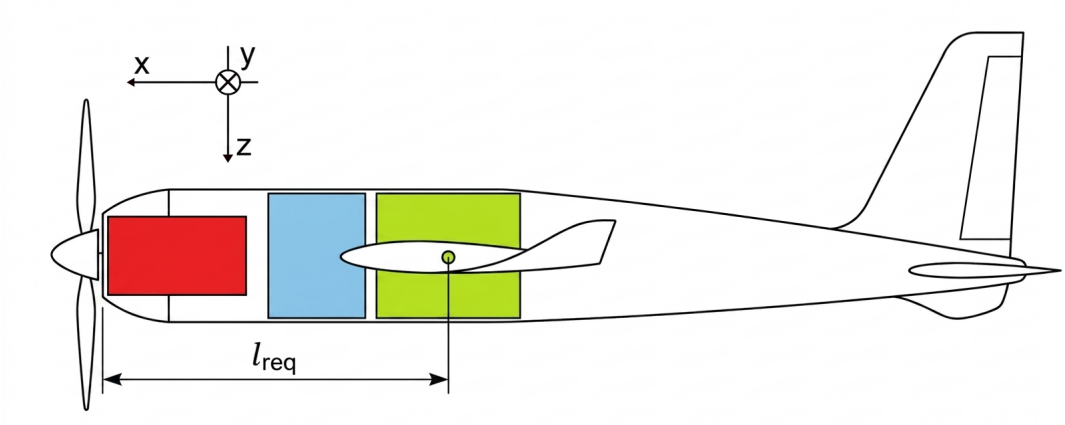


Figure 6 – Internal distribution of elements inside the UAV fuselage.

The engine is shown in red and is modeled as a rectangular prism with sides x, y, and z (length, width, and height, respectively). The payload, shown in blue, is modeled as a cylinder with a cross-section equal to that of the fuselage and a volume specified as an input parameter for the problem (the mass and the volume of the payload are requirements for the mission). Finally, the fuel tank is shown in green. This is also a cylinder with a diameter equal to that of the fuselage and a volume derived from calculations of the fuel mass required for the mission. Additionally, the fuel tank is centered on the half-chord of the main wing.
A first geometric constraint relates to the fuselage cross-section and requires that its diameter be equal to the diagonal of the engine, where $diag_{engine}$ is given by the sum of the y and z sides of the engine:

$$\sqrt{y_{eng}^2 + z_{eng}^2} \leq D_{fus} \tag{5}$$

The second constraint concerns the longitudinal footprint of the three components and requires that the length from the nose to the midpoint of the wing chord be equal to the length of the engine, plus the length of the payload volume and half the volume of the fuel tank:

$$l_{req} = 1.1 \left(x_{eng} + x_{payload} + \frac{x_{tank}}{2} \right) \leq l_{fus} \tag{6}$$

A length margin of 10% is considered in this study to account for the presence of other components and separation elements such as a firewall.

2.2.3 Final formulation

Table 2 summarizes the MDO problem formulation for the ICE-powered configuration. The objective function is the maximization of flight endurance t_{max}.

Table 2 – Mathematical formulation of the MDO for ICE-powered configurations.

	Parameter	Description
Design variables	k_{WS}	Sizing coefficient on the wing loading
	AR_w, AR_{ht}, AR_{vt}	Aspect ratios of the wing and tails
	λ_w	Taper ratio of the wing
	k_w	Sizing coefficient on the wing position
	k_t	Sizing coefficient on the tail moment arm
	$k_{y_{pro}}$	Sizing coefficient on the y-location of VTOL propellers
	$k_{h_{spar}}$	Sizing coefficient on the spars' height
	k_{arm}, k_{spar}	Aspect ratios of the arms and spars
	$\underline{x_{prop}}$	Set of design variables for the propulsion system
	k_M	Oversizing coefficient on the load mass
	$k_{C_{D_0}}$	Sizing coefficient on the parasitic drag coefficient
	k_S	Oversizing coefficient on the wing surface
Constraints	$W/S \leq (W/S)_{stall}$	Constraint on the stall speed
	$SM_{req} \leq SM$	Constraint on the static margin
	$V_{engine} + V_{tank} + V_{pay} \leq V_f$	Constraint on the fuselage volume
	$y_{pro}^{MR} \leq b_w/2$	Constraint on the maximum y-location of VTOL propellers
	$h_{spar} \leq t_{wing}$	Constraint on the spars' height
	$\sigma_{root}^{MR} \leq \sigma_{max}$	Constraint on the spars' bending stress during VTOL
	$\underline{g(x_{prop})} \leq 0$	Set of constraints for the propulsion system
	$m_{uav} \leq m_{uav,req}$	Constraint on the maximum total mass
	$m_{uav} \leq m_{uav,guess}$	Consistency constraint on the total mass
	$C_{D_0,guess} = C_{D_0}$	Consistency constraint on the parasitic drag coefficient
	$S_{top} \leq S_{top,guess}$	Consistency constraint on the top (projected) area
Objectives	t_{max}	Maximize flight endurance

Figure 7 shows the XDSM diagram ([22]) of the resulting MDO problem that now integrates the ICE module.

3. Endurance evaluation for different UAV architectures

This section compares the cruise endurance of four propulsion architectures, an electric multirotor (quadcopter), a hybrid VTOL, an electric fixed-wing and a thermal (internal-combustion) fixed-wing, across a range of MTOW and payload. The study is restricted to the small-UAV regulatory class, i.e. a maximum take-off mass (MTOM) of $25\,\mathrm{kg}$: this threshold is the ceiling of the EASA "Open" category [8] and, equivalently, of the FAA Part 107 small-UAS rule [9] ($55\,\mathrm{lb} \approx 25\,\mathrm{kg}$). It is the regime for which the FAST-UAV disciplinary models are calibrated. The airspeed to the design value of each category are $10\,\mathrm{m/s}$ for the multirotor and $16\,\mathrm{m/s}$ for the fixed-wing and hybrid VTOL platforms. For each (MTOW, payload) point the energy storage (battery or fuel) is sized to fill the take-off-mass budget so as to maximise the cruise endurance. All estimates refer to steady-state cruise.

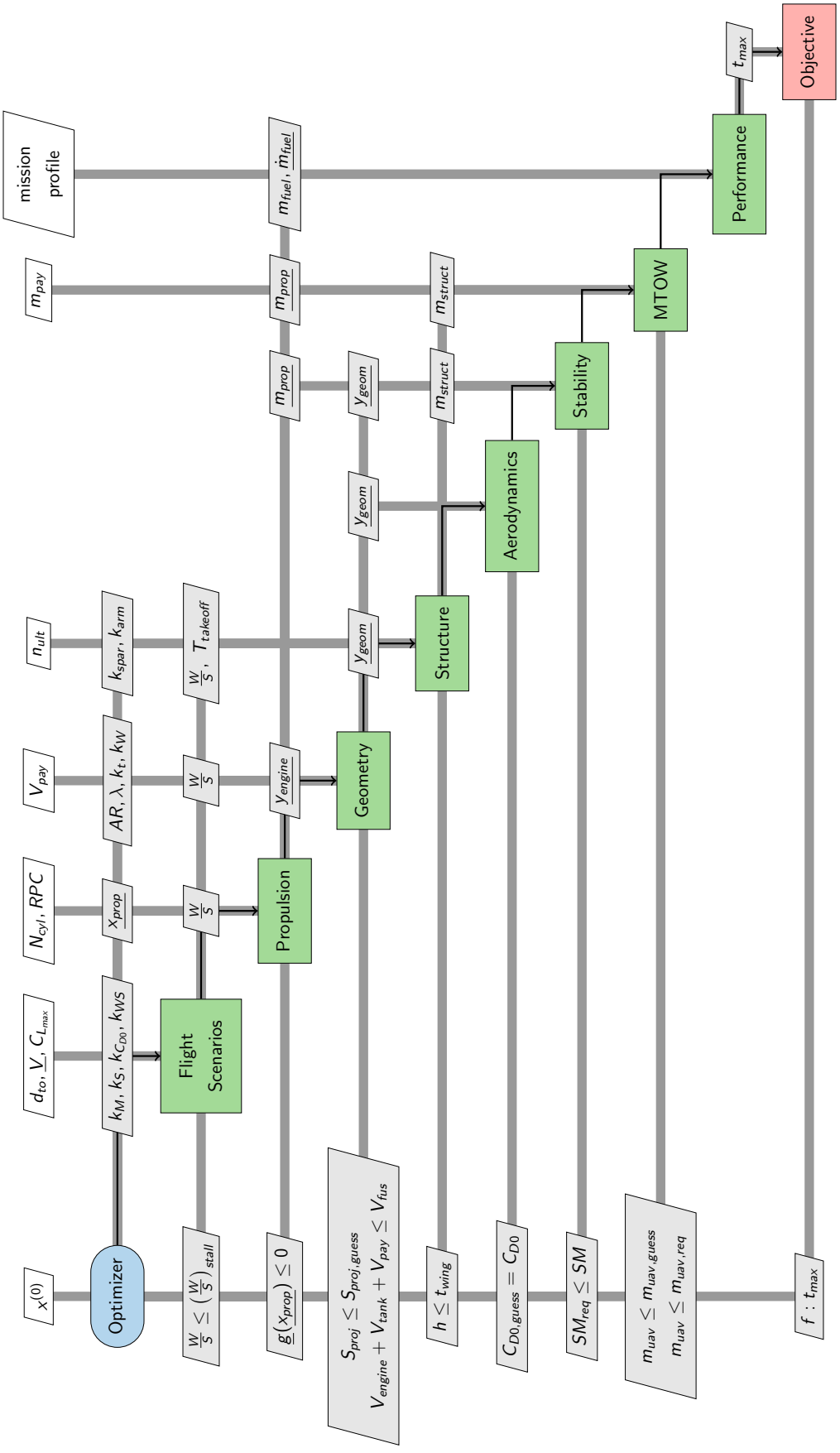


Figure 7 – XDSM diagram of the MDO problem implementing ICEs.

Table 3 – Cruise endurance (min) versus MTOW and payload for four propulsion architectures. "–" denotes unfeasible designs

MTOW	Payload	Quadcopter	Hybrid VTOL	Fixed-wing (el.)	Fixed-wing (th.)
5 kg	1 kg	31	126	202	–
5 kg	2 kg	16	28	88	–
10 kg	1 kg	41	176	266	665
10 kg	3 kg	26	87	159	383
10 kg	5 kg	12	–	45	–
15 kg	3 kg	33	119	211	727
15 kg	6 kg	18	23	91	386
15 kg	9 kg	5	–	–	–
20 kg	4 kg	31	109	208	717
20 kg	8 kg	17	–	85	383
20 kg	12 kg	–	–	–	–
25 kg	5 kg	30	100	204	705
25 kg	10 kg	15	–	81	374
25 kg	13 kg	8	–	–	163
25 kg	15 kg	–	–	–	–

Where it can be sized, the thermal fixed-wing consistently achieves the highest endurance, owing to the substantially higher specific energy of hydrocarbon fuels compared with lithium cells: at light payload it exceeds the electric fixed-wing by roughly a factor of three, the hybrid VTOL by a factor of six, and the multirotor by more than an order of magnitude (e.g. 727 vs 211 vs 119 vs $33\,\mathrm{min}$ at $15\,\mathrm{kg}$ / $3\,\mathrm{kg}$). The ranking thermal fixed-wing $>$ electric fixed-wing $>$ hybrid VTOL $>$ multirotor holds throughout the grid: the hybrid VTOL recovers the cruise efficiency of a fixed wing relative to the multirotor, but a permanent penalty for its vertical-lift hardware keeps it below the pure electric fixed-wing.

The thermal fixed-wing, however, cannot be sized below about $10\,\mathrm{kg}$ MTOW: the smallest engine in the regression database is rated at $1.6\,\mathrm{kW}$, disproportionately large for a sub-$10\,\mathrm{kg}$ airframe, so the corresponding cells are empty. In this micro/mini regime only the electric architectures remain feasible, the electric fixed-wing dominating ($202\,\mathrm{min}$ at $5\,\mathrm{kg}$ / $1\,\mathrm{kg}$).

At constant MTOW the endurance decreases monotonically with payload, since the additional payload directly displaces stored energy at fixed gross weight, and at constant payload it increases with MTOW, as a larger airframe affords a more favourable energy-to-mass fraction. Beyond a payload fraction of roughly 50–60% no architecture remains feasible, and the architectures reach this limit in a definite order: the hybrid VTOL first – its lift hardware leaving the least mass margin – then the electric fixed-wing, and finally the thermal fixed-wing and the multirotor; a $15\,\mathrm{kg}$ payload is unattainable anywhere within the $25\,\mathrm{kg}$ envelope.

4. Conclusion

This paper presented the extension of the FAST-UAV multidisciplinary design optimization framework to internal combustion engine (ICE) propulsion, enabling a consistent comparison of the cruise endurance of a thermal fixed-wing, an electric fixed-wing, a hybrid VTOL and an electric multirotor over a range of MTOW and payload combinations.

A set of data regression models for two-stroke ICEs was developed from manufacturer catalogs covering single-, two-, and four-cylinder configurations, with maximum power between $1.6\,\mathrm{kW}$ and $46.3\,\mathrm{kW}$. These models, together with a thermodynamic-cycle description and a fuel-consumption model whose conversion efficiencies are calibrated to the small-engine size class, were integrated as a fully coupled discipline within the NVH-based MDO formulation.

The endurance evaluation, carried out within the small-UAV regulatory class (maximum take-off mass below $25\,\mathrm{kg}$), confirmed that the thermal fixed-wing configuration consistently achieves the highest endurance wherever it can be sized, ranging from approximately $163\,\mathrm{min}$ to $727\,\mathrm{min}$: it exceeds the electric fixed-wing by roughly a factor of three, the hybrid VTOL by a factor of six, and the electric multirotor by more than an order of magnitude, owing to the substantially higher specific energy of hydrocarbon fuels compared to lithium-polymer batteries. Below about $10\,\mathrm{kg}$ MTOW, however, the

thermal option is unavailable – the smallest catalogued engine being oversized for the airframe – leaving the electric architectures as the only feasible choice in the micro/mini class. The analysis also delimited the feasible design space, no architecture being able to carry a payload above roughly 50–60% of its MTOW, the hybrid VTOL reaching this limit first owing to its vertical-lift hardware.
Several areas for improvement have been identified. The four-cylinder engine regression models, while exhibiting high R-squared values, are supported by a limited sample size; expanding the dataset would consolidate their statistical robustness and generalizability. Extending the propulsion module to four-stroke engines would also broaden the architectural trade space toward the higher power ranges typical of ultralight aircraft applications. The fuel consumption is currently derived from a constant brake efficiency; replacing it with an operating-point-dependent specific-fuel-consumption map, together with a propeller-efficiency map, would capture the higher part-load consumption and refine the absolute endurance estimates. In the same vein, the engine mass currently regresses on power alone, so single- and two-cylinder engines of equal power are indistinguishable in mass; resolving this would sharpen the comparison at the upper end of the size range. Finally, adopting a more representative fuel-tank model and conducting a systematic sensitivity analysis are left for future work to quantify the robustness of the FAST-UAV framework with respect to variations in its key modelling and propulsion-related assumptions.

Copyright Statement

The authors confirm that they, and/or their company or organization, hold copyright on all of the original material included in this paper.
The authors also confirm that they have obtained permission, from the copyright holder of any third party material included in this paper, to publish it as part of their paper. The authors confirm that they give permission, or have obtained permission from the copyright holder of this paper, for the publication and distribution of this paper as part of the ICAS proceedings or as individual off-prints from the proceedings.

References

[1] Joaquim R. R. A. Martins and Andrew Ning. *Engineering design optimization*. Cambridge University Press, Cambridge, 2022.

[2] A. Salas and J. Townsend. Framework requirements for MDO application development. In *7th AIAA/USAF/NASA/ISSMO Symposium on Multidisciplinary Analysis and Optimization*, St. Louis,MO,U.S.A., September 1998. American Institute of Aeronautics and Astronautics.

[3] Félix Pollet, Scott Delbecq, Marc Budinger, Jean-Marc Moschetta, and Jonathan Liscouët. A common framework for the design optimization of fixed-wing, multicopter and vtol uav configurations. In *33rd Congress of the International Council of the Aeronautical Sciences*, Stockholm, Sweden, September 2022.

[4] Félix Pollet. *Design Optimization of Unmanned Aerial Vehicles: A Multidisciplinary Approach with Uncertainty, Fault-Tolerance, and Environmental Impact Assessments*. Ph.D. Thesis, ISAE-SUPAERO, Toulouse, France, 2024.

[5] Hang Zhang, Tao Xiang, Shenwei Zhang, and Wei Wang. Multidisciplinary Design Optimization of the Vertical Takeoff and Landing for Fixed-Wing Hybrid Unmanned Aerial Vehicles. *Journal of Aerospace Engineering*, 39(2):04025129, March 2026.

[6] Martin J. Muir, Edward J. Kolb, Aaron T. Parkinson, Graham A. Robertson, Carl L. Muldal, Osvaldo Querin, Robert W. Hewson, and Vassili Toropov. The Use of MDO and Advanced Manufacturing to Demonstrate Rapid, Agile Construction of a Mission Optimized UAV. In *54th AIAA/ASME/ASCE/AHS/ASC Structures, Structural Dynamics, and Materials Conference*, Boston, Massachusetts, April 2013. American Institute of Aeronautics and Astronautics.

[7] Maria Luiza Cassâo Gatelli, Carlos Eduardo De Souza, and Marcos Daniel De Freitas Awruch. A study for a MDO Process Applied to Conceptual Design of a Remotely Piloted Aircraft. pages 45–55, October 2019.

[8] European Union. Commission implementing regulation (EU) 2019/947 on the rules and procedures for the operation of unmanned aircraft. Official Journal of the European Union, L 152, pp. 45–71, 2019. Defines the “Open” category, applicable to unmanned aircraft with a maximum take-off mass below 25 kg.

[9] Federal Aviation Administration. 14 CFR part 107 — small unmanned aircraft systems. Operation and

Certification of Small Unmanned Aircraft Systems, Federal Register, vol. 81, no. 124, pp. 42064–42214, 2016. Defines a small unmanned aircraft as weighing less than 55 lb (25 kg) on take-off.

[10] Justin S. Gray, John T. Hwang, Joaquim R. R. A. Martins, Kenneth T. Moore, and Bret A. Naylor. OpenMDAO: an open-source framework for multidisciplinary design, analysis, and optimization. *Structural and Multidisciplinary Optimization*, 59(4):1075–1104, April 2019.

[11] Christophe David, Scott Delbecq, Sebastien Defoort, Peter Schmollgruber, Emmanuel Benard, and Valerie Pommier-Budinger. From fast to fast-oad: An open source framework for rapid overall aircraft design. *IOP Conference Series: Materials Science and Engineering*, 1024(1):012062, jan 2021.

[12] Aurélien Reysset, Marc Budinger, and Jean-Charles Maré. Computer-aided definition of sizing procedures and optimization problems of mechatronic systems. *Concurrent Engineering*, 23(4):320–332, 2015.

[13] Scott Delbecq, Marc Budinger, and Aurélien Reysset. Benchmarking of monolithic mdo formulations and derivative computation techniques using openmdao. *Struct. Multidiscip. Optim.*, 62(2):645–666, August 2020.

[14] R. J. Balling and J. Sobieszczanski-Sobieski. Optimization of coupled systems - a critical overview of approaches. *AIAA Journal*, 34(1):6–17, 1996.

[15] Scott Delbecq. *Knowledge-based multidisciplinary sizing and optimization of embedded mechatronic systems-application to aerospace electro-mechanical actuation systems*. PhD thesis, INSA de Toulouse, 2018.

[16] Snorri Gudmundsson. *General aviation aircraft design: applied methods and procedures*. Butterworth-Heinemann, an imprint of Elsevier, Oxford Cambridge, second edition edition, 2022.

[17] Joseph K. Ausserer, Marc D. Polanka, Jacob A. Baranski, Keith D. Grinstead, and Paul J. Litke. Measurement of Loss Pathways in Small, Two-Stroke Internal-Combustion Engines. *SAE International Journal of Engines*, 10(2):128–143, March 2017.

[18] S. Menon and Christopher P. Cadou. Scaling of Miniature Piston-Engine Performance, Part 1: Overall Engine Performance. *Journal of Propulsion and Power*, 29(4):774–787, July 2013.

[19] S. Menon and Christopher P. Cadou. Scaling of Miniature Piston Engine Performance Part 2: Energy Losses. *Journal of Propulsion and Power*, 29(4):788–799, July 2013.

[20] Gordon Blair. *Design and Simulation of Two-Stroke Engines*. SAE International, Warrendale, 1st ed edition, 1996.

[21] John Heywood. *Internal Combustion Engine Fundamentals 2E*. McGraw-Hill Education, New York, N.Y, 2nd edition edition, 2019.

[22] Andrew B. Lambe and Joaquim R. R. A. Martins. Extensions to the design structure matrix for the description of multidisciplinary design, analysis, and optimization processes. *Structural and Multidisciplinary Optimization*, 46(2):273–284, August 2012.